Physicochem. Probl. Miner. Process., 57(6), 2021, 113-126

http://www.journalssystem.com/ppmp

Physicochemical Problems of Mineral Processing

ISSN 1643-1049

Received August 13; reviewed; accepted October 16

Flotation separation of dolomite and apatite using polyaspartic acid as inhibitor

Yuntao Kang [1], Qin Zhang [2,3,4]

[1] College of Mining, Guizhou University, Guiyang 550025, China

[2] Guizhou Academy of Sciences, Guiyang, 550001

[3] National & Local Joint Laboratory of Engineering for Effective Utilization of Regional Mineral Resources from Karst Areas, Guiyang, Guizhou, 550025, China

[4] Guizhou Key Laboratory of Comprehensive Utilization of Non-metallic Mineral Resources, Guiyang 550025, China

Corresponding author: zq6736@163.com (Qin Zhang)

Abstract: In this paper, polyaspartic acid (PASP) was exploited as a novel dolomite depressant for flotation separation of apatite and dolomite. A series of tests with Zeta potential, FTIR and XPS were used to reveal the inhibitory mechanism of PASP on dolomite. The microflotation test illustrated that PASP has a strong inhibitory impact on dolomite, and little effect on the floatability of apatite in the pH range of 9-11. When using 2.7 Mg/L PASP as the depressant under sodium oleate (NaOl) system, the flotation recovery of dolomite dropped dramatically to 9.95%, and the recovery of apatite remained at about 88.27% at pH 10. Both dolomite and apatite have calcium ion on the surface. The calcium ion on the surface of apatite were strongly inhibited and repelled by the localized anions, while the important role on the surface of dolomite was positively charged magnesium ion and localized calcium species. PASP could ionize carboxylate ion under alkaline conditions, which could chemically chelate with the exposed metal ion and be adsorbed on the surface of dolomite. And then prevent the further adsorption of NaOl onto dolomite, which greatly weaken the floatability of dolomite and enhanced the flotation separation of the two minerals.

Keywords: dolomite, apatite, polyaspartic acid, flotation, inhibitory mechanism

1. Introduction

Phosphate ore is the important raw material for production of phosphorus, which is widely applied in agriculture, chemical industry, national defense, and food processing (Liu et al., 2017). Phosphate-containing minerals in nature mainly exist in the form of fluorapatite, followed by hydroxyapatite and chlorapatite. The common associated gangue minerals contained in phosphate ore are iron oxide, clay minerals, silicate minerals and carbonate minerals (calcite and dolomite, etc.) (Amirech et al., 2018).Due to the co-existence of apatite and these gangue minerals, high-quality phosphate resources become less and less. Especially in China, more than 90% of phosphate ore resources belong to middle-low grade phosphate ore with an average grade of about 17% (Zhong et al., 2009).Therefore, it is necessary to further strengthen the mineral separation and utilization of middle-low grade phosphate ore.

There are lots of methods for beneficiation of phosphate ore, including heavy medium separation method (Wang and Zhang, 2010),calcination method (Zhou et al., 2019),leaching method (Gharabaghi et al., 2010)and flotation method (Ye et al., 2018).Flotation is an effective separation technology for low-grade phosphate ore (Abouzeid, 2008), which mainly uses the difference in the physical and chemical properties of the mineral surface to selectively separate apatite from gangue minerals with flotation reagents (Dong et al., 2020).Since the surface active sites of apatite and carbonate mineral are similar for phosphate ore (Wang et al., 2020),the dissolved metal ions of carbonate or apatite could be

DOI: 10.37190/ppmp/143128

adsorbed on the surface of the two minerals during the flotation process (Hoang et al., 2018),which makes it difficult to separate the two minerals effectively. In addition, the localized anion dissolved on the surface of apatite and dolomite exist steric hindrance (Cao et al., 2019). The two minerals could be affected by surface dissolved ions and undergo surface transformation with suitable pH conditions, resulting in closer surface properties，which further increase the difficulty of flotation separation of the two minerals (Li et al., 2017). In the flotation system of calcium-magnesium phosphate ore, fine-grained dolomite is easily attached to bubbles or entrained into the phosphate concentrate (Hoang et al., 2019), which seriously decreases the quality level of beneficiation products (Yang et al., 2019; Chen et al., 2020). In summary, the flotation of calcium-magnesium phosphate ore is greatly affected by the crystal structure of minerals and surface dissolved ions，making it difficult for traditional flotation reagents to effectively separate the two minerals. Therefore, the development and utilization of high-efficiency flotation reagents is a significant step for flotation of calcium-magnesium phosphate ore.

Collector is one of the most critical factors for flotation (Li et al., 2017). Traditional fatty acid agents, such as oleic acid or oleate (Xie et al., 2018; Wang et al., 2020), waste oil fatty acid (Yu et al., 2018) and mixed collectors (Cao et al., 2015) are of importance in the flotation of calcium-magnesium phosphate ore due to their wide sources and low prices (Sis and Chander 2003). Since fatty acid agents are non-selectively adsorbed on the surface of apatite and dolomite (Filippova et al., 2018), it is difficult to effectively separate the two minerals without inhibitors. In addition, as fatty acid collectors have poor solubility under normal temperature conditions and are used with dosage of reagent together in industrial production, the synthesis and use of new collectors have been attached importance, including hybrid collectors (Cao et al.,2015; Aline et al.,2019), alkyl hydroxamic acid (Yu et al., 2016), oleic acid amide (Jong et al.,2017), sodium dodecyl sulfate (Sun et al., 2017) and N-hexadecanoylglycine (Cao et al., 2019) etc. These collectors reduce the dosage of inhibitor acid to a certain extent, increasing the difference in floatability of apatite and dolomite. But the collectors have complex synthesis processes, high costs, poor applicability, low selectivity, poor environmental protection and other shortcomings, making it difficult to completely replace traditional fatty acid collectors. It can be seen that the new collectors have certain limitations in the flotation of phosphate ore. Therefore, the development and utilization of inhibitors is the key to improving the flotation separation of apatite and dolomite.

Inhibitors selectively increase the hydrophilicity of mineral surfaces through the action of agents to enhance the difference in floatability between apatite and gangue minerals (dolomite, calcite, and quartz). Phosphoric acid (Liu et al., 2017; Kaba et al., 2021), sodium pyrophosphate (Pan et al.,2020), 2-phosphonobutane-1,2,4-tricarboxylic acid (Yang et al., 2020) and other phosphorus-containing inhibitors are routinely used in the flotation of phosphate ore. Phosphoric acid and mixed acids (Liu et al.,2017) (phosphoric acid and sulfuric acid) are widely applied to industrial production. Although these acids can effectively inhibit apatite, excessive application can cause numerous challenges such as higher flotation costs, corrosion of flotation equipment, and serious water pollution (Shakoor et al.,2021). Recently, several organic inhibitors have been exploited as dolomite inhibitors for the flotation separation of apatite and dolomite, such as acrylic acid-2-acrylamido-2-methylpropanesulfonic acid copolymer (Yang et al., 2020), (poly(acrylic acid-co-maleic acid) sodium salt (Yang et al., 2020) , hydrolytic polymaleic anhydride (Yang et al., 2021), xanthan gum (Zeng et al., 2021) and so on. These organic inhibitors are environmentally friendly, highly selective, non-toxic, etc. However, these agents are currently limited to laboratories because of synthesis cost. Therefore, the development of environmentally friendly, efficient and low-cost new inhibitors can beneficial to boosting the development and utilization of phosphate ore.

Polyaspartic acid (PASP) is a water-soluble amino acid polymer, which has the advantages in being non-toxic, easily degradable, mature in synthetic process and available (Yang et al., 2020). Since PASP contains a large number of active groups such as carboxyl and amide groups chelating with metal ion in Fig. 1 (Yang et al.2015), it has good scale and corrosion inhibition properties (Chen et al., 2018; Liu et al., 2011). Therefore, PASP is often applied as a dispersant and scale inhibitor for the water treatment. Chen et al., (Chen et al., 2019) compared the inhibitory effects of polyhydroxy acids such as PASP in the flotation of calcite. Wei et al., (Wei et al., 2020) used PASP as an inhibitor to effectively separate calcite and scheelite. These studies indicated that the dissolved carboxyl groups of PASP

could chelate with the calcium ion on the surface of calcite, promoting the flotation separation of calcite and scheelite. Both calcite and dolomite are calcium-containing minerals with similar calcium points on the surface, which provides a possibility for PASP as a depressant for flotation separation of apatite and dolomite.

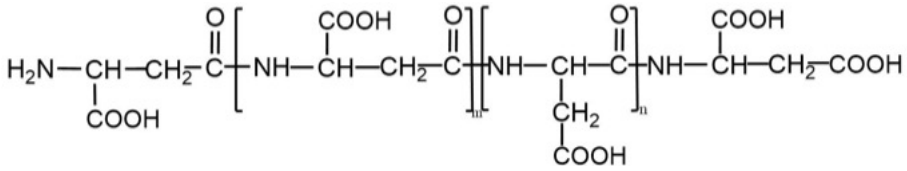

Fig. 1. Chemical structure of PASP repeat unit

In this paper，the PASP was regarded as a new depressant for flotation separation of apatite and dolomite under sodium oleate (NaOl) system. The flotation behaviors of dolomite and apatite in different flotation reagent systems were studied through microflotation experiments. Combined with the detection of Zeta potential, Fourier transform infrared spectroscopy (FTIR) and X-ray photoelectron spectroscopy (XPS), the selective adsorption mechanism of PASP onto apatite and dolomite was discussed. Finally, a flotation separation model of the two minerals under the action of PASP was proposed, which intuitively reflected the inhibition mechanism of PASP on dolomite during the flotation process.

2. Materials and methods

2.1. Materials

The pure mineral samples (dolomite and apatite) used in the experiment were collected from Guizhou Province, China. The raw ore was crushed with a hammer and picked up by hand, then the selected small samples were placed in a ceramic mill for grinding. The ground samples were screened with a standard screen mesh to obtain samples with different particle sizes. Among them, the samples with a particle size of 75-37 μm was used for microflotation experiments, and sample with a particle size of less than 37 μm was further ground to 13 μm with agate to analyze by FTIR, Zeta potential, and XPS. As shown in Fig. 2, the results of X-ray diffraction (XRD) revealed that apatite and dolomite had higher purity and no obvious impurities. The chemical compositions of dolomite and apatite are shown in Table 1, it was confirmed that the purity of dolomite and apatite are 92.15% and 91.32%, respectively, which met the experimental requirements. During the experiment, analytical grade NaOl and chemical grade PASP with purity of 95% and 99% were purchased from Macleans Reagent Co. Ltd. The slurry pH was adjusted with 0.1 mol/L hydrochloric acid (HCl) and 0.1 mol/L sodium hydroxide (NaOH). During the experiment, standard deionized water was used to prepare fresh stock solutions every day, including medicament solution and floating water.

2.2. Micro-flotation test

The microflotation flow was depicted in Fig. 3. The single mineral flotation test was carried out using the microflotation test method. In the experiment, the XFGC flotation machine (Jilin Exploration Equipment Co., Ltd., Changchun) was used. The flotation cell capacity was 40 cm^3, and the impeller speed was adjusted to 1992 r/min. 2.0 g of mineral samples and 35 cm^3 of deionized water were added to the flotation cell. The slurry was evenly stirred for 1 min，followed by adding PASP for 2 min. After adjusting to appropriate pH with HCl or NaOH solution，NaOl was added for 2 min. Then the flotation was performed for 5 min. The flotation products were filtered, dried and weighed, and the recovery was calculated. The flotation test was repeated 3 times with the same conditions. The average value was taken as the final result, and the standard deviation was taken as the error bar.

$$\varepsilon\iota = \frac{M_1}{M_1+M_2} \tag{1}$$

where ε is the recovery of minerals; M_1 and M_2 represent the weight (g) of concentrate products and tailings, respectively

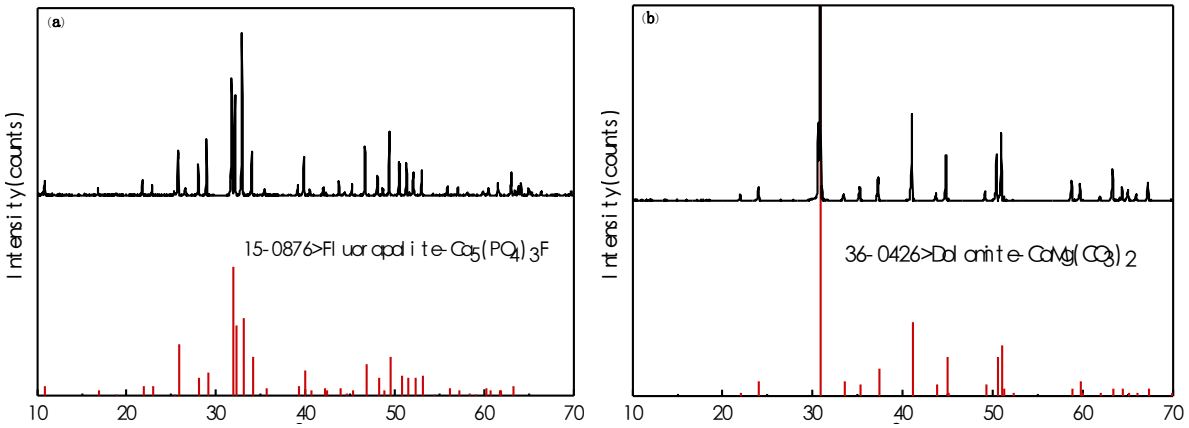

Fig. 2. X-ray diffraction patterns of apatite (a) and dolomite (b) samples

Table 1. Multi-composition analysis result of dolomite and apatite

Minerals	Compositions (wt. %)						
	P_5O_2	MgO	SiO_2	CaO	Al_3O_2	Fe_2O_3	F
Apatite	37.443	0.044	3.286	54.93	0.237	0.214	2.039
Dolomite	0.073	20.180	0.383	30.27	0.060	0.153	0.019

2.3. Zeta potential experiments

A Coulter Delsa 440sx Zeta potential analyzer was used to measure the Zeta potential of apatite and dolomite under different flotation systems, and the particle size of the mineral sample in the experiment was less than 13 μm .40 Mg of mineral sample and 40 ml of potassium nitrate solution were added in a 50 cm^3 beaker. The dilute HCl solution and NaOH solution were used to adjust the slurry pH. A certain dosage of reagents was added at a conditioning time of 3 min, and the mineral sample was kept uniformly dispersed for a certain period of time using ultrasound. The suspension was left to stand for another 3 min to allow the larger particles to settle, then the supernatant in beaker was carried to the electrode tank to measure its Zeta potential. Each measure was repeated 3 times, and the average value was taken as the final result. The standard deviation was taken as the error bar. The electrolyte used in the test was a 10^{-3} mol/LKNO_3 solution, and all measurements were performed at about 25 °C.

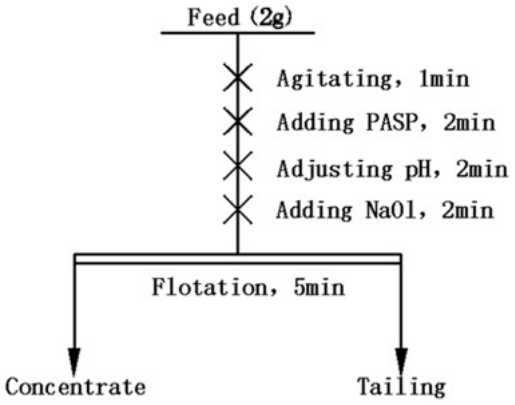

Fig. 3. Flow chart of flotation test

2.4. FTIR analysis

Nicolet 670 (USA) was used to perform infrared spectroscopy analysis for samples of apatite and dolomite with and without treatment with different reagents. 0.5 g of sample and different flotation reagents were added in flotation cell and stirred for 30 min. Then, the samples were filtered and

washed with deionized water for 3 times, dried in an oven for 24 hours. The experiment was worked with KBr tableting method in transmission mode. The range of wavelength was 4000-400 cm^{-1}.After calibrating by measuring the background peak of KBr itself, the uniformly mix 100 Mg KBr sample with 1.0 Mg mineral sample were pressed into tablets to measure the infrared spectrum.

2.5. XPS analysis

The preparation method of test sample followed the flotation process. The samples with particle size less than 5 um were treated by flotation reagent .The samples prepared by flotation were filtered, rinsed with deionized water and dried. The XPS measuring equipment for mineral samples was Thermo Scientific K-Alpha. The relevant parameters are as follows: Color Al-Ka X-ray source (150 W), energy steps of 1.000 eV (scanning spectrum) and 0.050 eV (high resolution spectrum).The test results were based on the C1s standard absorption peak, and the advantage fitting software was used to perform charge correction on the spectra of different elements. The measured data was further analyzed by the separated peaks and peak fitting of the scan spectrum.

3. Results and discussion

3.1. Micro-flotation experimental results

The effects of pH, NaOl dosage and PASP dosage on the flotation behavior of apatite and dolomite are shown in Fig. 4. Fig. 4 (a) depicted the recovery of apatite and dolomite with different pH conditions, and the dosage of NaOl was set at 160 Mg/L. The floatability difference of apatite and dolomite was quite narrow in the pH range of 4-12, and the recovery was higher than 80%. However, there was a slight distinction in the overall recovery of the two minerals. The recovery of apatite rose slowly and then slightly decreased in the pH range of 4-12, while the recovery of dolomite was generally fluctuating. The floatability difference between the two minerals was the smallest at pH 6 and 9. The overall difference between the recovery of the two minerals varied from 0.29% to 6.74%, which was not enough to achieve effective separation. Taking into account the maximum flotation recovery of apatite, the pH value selected in the following experiment would be 10.

The recovery changes of apatite and dolomite with different dosage of NaOl is shown in Fig. 4 (b). With the enhancement of the NaOl dosage, the recovery of the two minerals increase significantly at pH 10. When the dosage of NaOl was 160 Mg/L, the recovery of both apatite and dolomite are higher than 95%. This trendy revealed that NaOl had a strong collection ability for dolomite and apatite, but the selectivity was relatively poor. Therefore, it was impossible to effectively separate the two minerals with a single NaOl. Considering the maximum recovery of apatite, the dosage of NaOl in the following experiments would be set as160 Mg/L.

Fig. 4 (c) describes the recovery curve of apatite and dolomite at different pH values after adding a certain dosage of collector and inhibitor. The dosages of NaOl and PASP were 160 Mg/L and 2.7 Mg/L, respectively. The variation showed that the recovery of apatite increased from 71.18% to 88.27% in the pH range of 6-10, and then it decreased slowly in the pH range of 10-12. Compared with apatite treated only by NaOl, the addition of NaOl and PASP had no significant impact on the recovery of apatite, which demonstrated that PASP had a weaker inhibitory effect on apatite. On the contrary, the recovery of dolomite treated with PASP dropped sharply from 86.07% to 14.63% in the pH range of 6-8, and slowly decreased in the pH range of 8-11.5. The recovery of dolomite droped to the lowest point of 9.98% at pH 10. It could be obtained that the optimal pH value for effective flotation separation of apatite and dolomite was 10.

Fig. 4 (d) depicts the effect of PASP dosage on the recovery of apatite and dolomite at pH 10 and the dosage of NaOl is 160 Mg/L. As shown in Fig. 4 (d), with the increase in the dosage of PASP from 0 to 2.7 Mg/L, the corresponding recovery of dolomite dropped dramatically from 95.78% to 9.95%. On the contrary, when the dosage of PASP was increased to 2.7 Mg/L, the recovery of apatite decreased by 7.22%. At this time, the floatability difference between the two minerals was the largest. Therefore, the optimal dosage of PASP as the inhibitor was 2.7 Mg/L.

In summary, the flotation separation of dolomite and apatite could be achieved under the combined action of PASP and NaOl in the pH range of 9-11. In contrast, the application range of

traditional acids (phosphoric acid, sulfuric acid) for phosphate ore flotation was limited to a narrow range at pH (Ruan et al., 2019). The experimental results indicated that, PASP could achieve the flotation separation of dolomite and apatite.

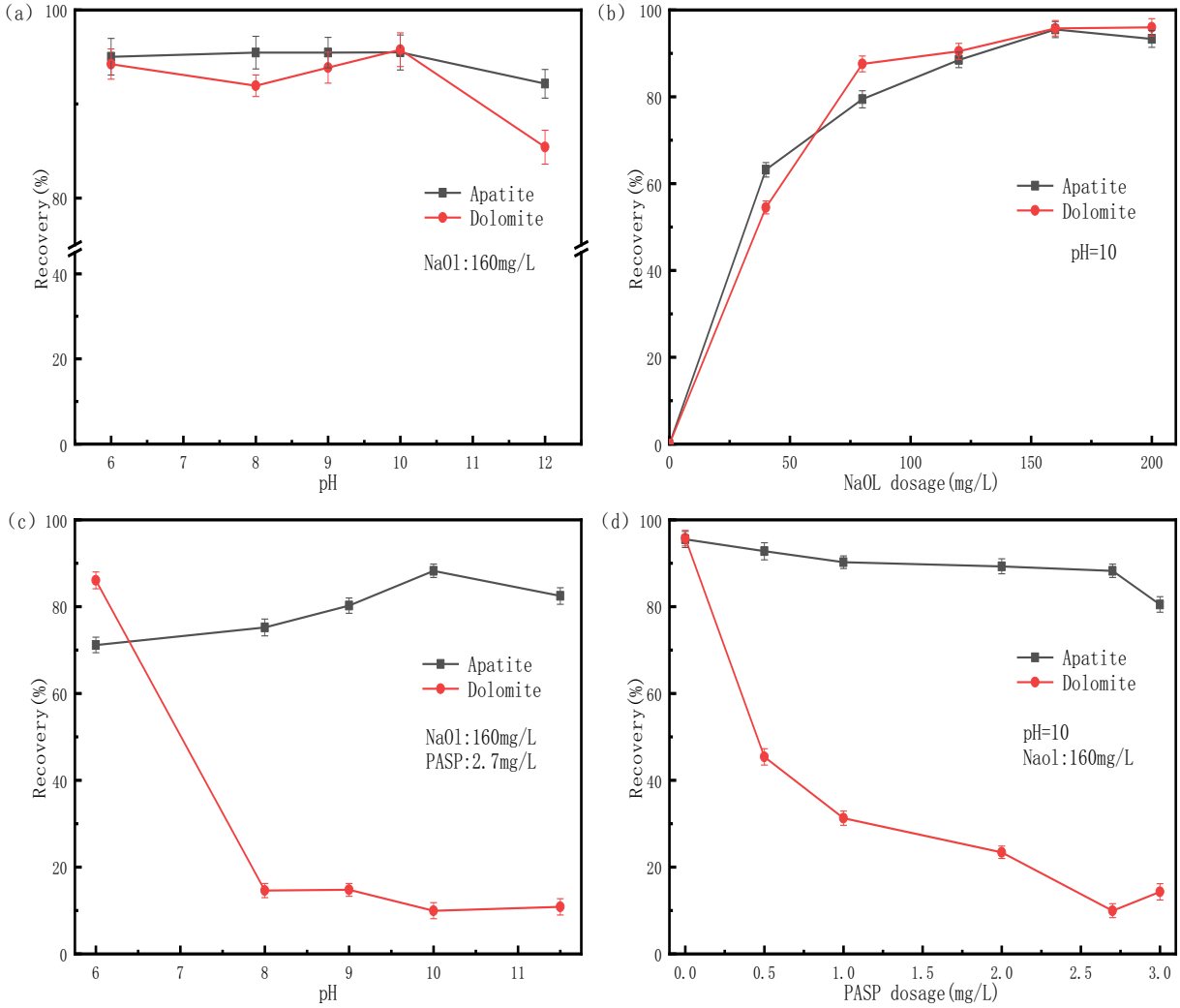

Fig. 4. (a, c) The influence of pH value with and without PASP, (b) NaOl dosage and (d) PASP dosage on the recovery of apatite and dolomite

3.2. Zeta potential analysis

Fig. 5 depicts the changeable trend of Zeta potential of dolomite and apatite with and without the action of PASP and NaOl at different slurry pH. In the pH range of 6-12，the Zeta potential of pure dolomite and apatite decreased with the increase of pH, and neither mineral had an isoelectric point. This is also consistent with previous research (Yang et al., 2020). The discrepancy was that the Zeta potential of dolomite treated by PASP was significantly reduced in the pH range of 9-12. It showed that the effect of PASP on the surface of apatite was weaker than that of dolomite in this interval. When PASP and NaOl were added at the same time, the changing trend of Zeta potential of dolomite was consistent with that of dolomite pretreated by PASP. And in the pH range of 8-12, the Zeta potential discrepancy between apatite with and without the action of PASP was quite narrow. Compared with dolomite, the Zeta potential of apatite with PASP pretreatment was significantly lower than that of dolomite. When the pH was 10, the difference in surface potential between dolomite with and without the action of PASP reached 13.14 mV, which indicated that the interacted effect of PASP and NaOl on the surface of dolomite was stronger. In other words, PASP would preferentially work on the surface of dolomite and hinder the adsorption of NaOl, while the apatite treated with PASP in advance had little effect on the further adsorption of NaOl. It can also be

confirmed from the changes of the Zeta potential of the two minerals treated with single NaOl. The Zeta potential of apatite with the combined action of PASP and NaOl was basically similar to that of apatite with treatment of single NaOl. In consequence, for the single mineral pretreated by PASP and NaOl, the NaOl in the pulp was mainly adsorbed on the surface of apatite, and the PASP in the pulp was mainly adsorbed on the surface of dolomite.

In order to further explore the competitive adsorption of PASP and NaOl on the surface of dolomite and apatite, the Zeta potential changes of the two minerals pretreated with different dosage of NaOl were tested. As shown in Fig. 5 (c), as the increase of NaOl dosage, the Zeta potential of dolomite and apatite had a downward trend, indicating that NaOl and PASP were adsorbed with a certain degree on the surface of dolomite and apatite. When the dosage of NaOl was in the range of 0-160 Mg/L, the Zeta potential discrepancy of dolomite was only 1.43 mV, showing that PASP prevented the adsorption of NaOl on the surface of dolomite. In comparison, the changing value of Zeta potential on the surface of apatite was 13.17 mV, illustrating that PASP had little effect on the adsorption of NaOl on the surface of apatite. These results all demonstrated that NaOl and PASP would have competitive adsorption on the surface of minerals when two agents existed at the same time. In other words, the adsorption of NaOl onto apatite was mainly NaOl, and the adsorption of PASP onto dolomite was mainly PASP.

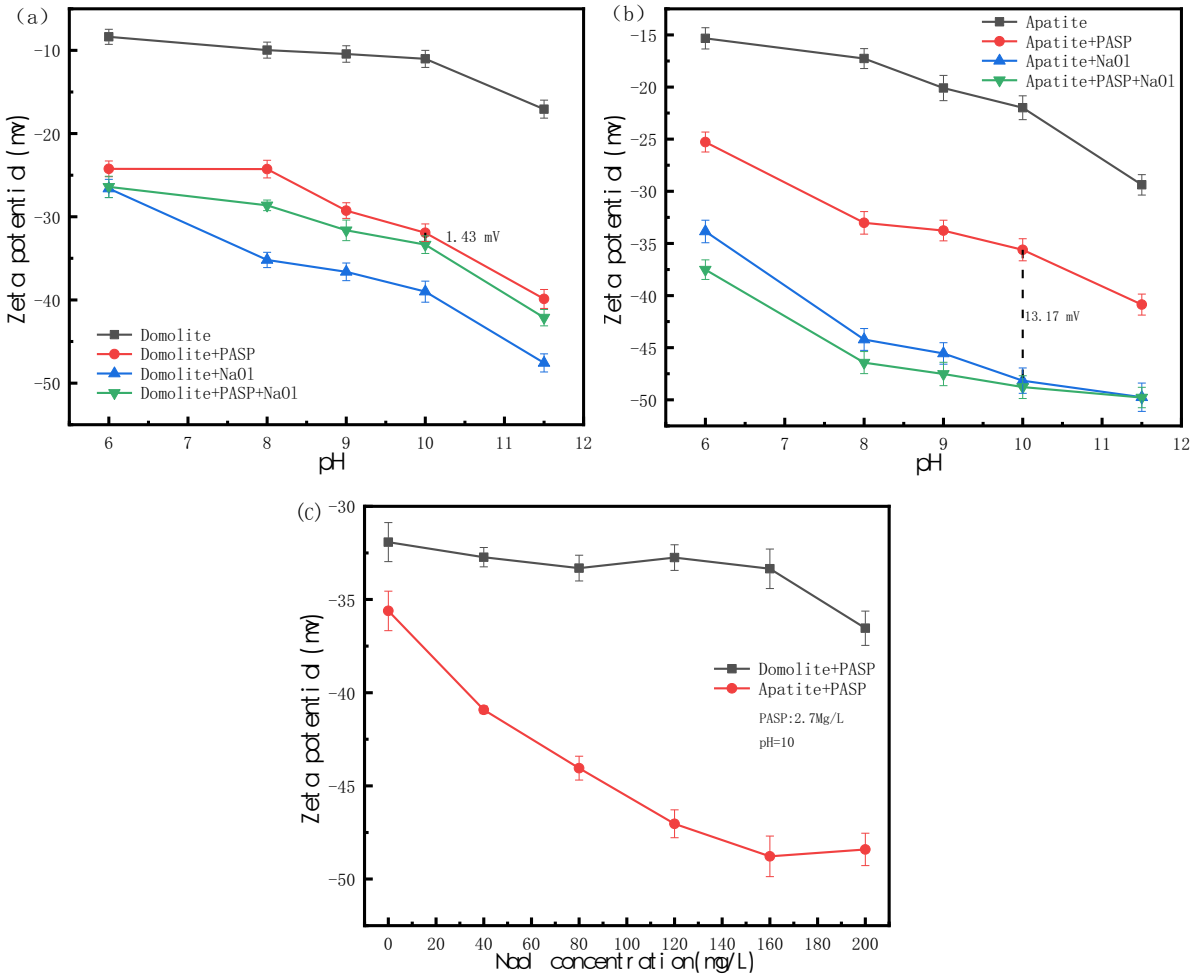

Fig. 5. Zeta potential values for dolomite (a), apatite (b) and dolomite and apatite (c) as a functin of pH, NaOl and PASP concentrations

3.3. FTIR analysis

FTIR is an effective method to characterize and detect molecular clusters and agent adsorption, which is often used to study the mechanism of agent action on minerals (Zhang et al., 2021). Fig. 6 is the spectrum of PASP. As shown in Fig. 6, there was a strong and broad absorption peak at 3454.56 cm^{-1},

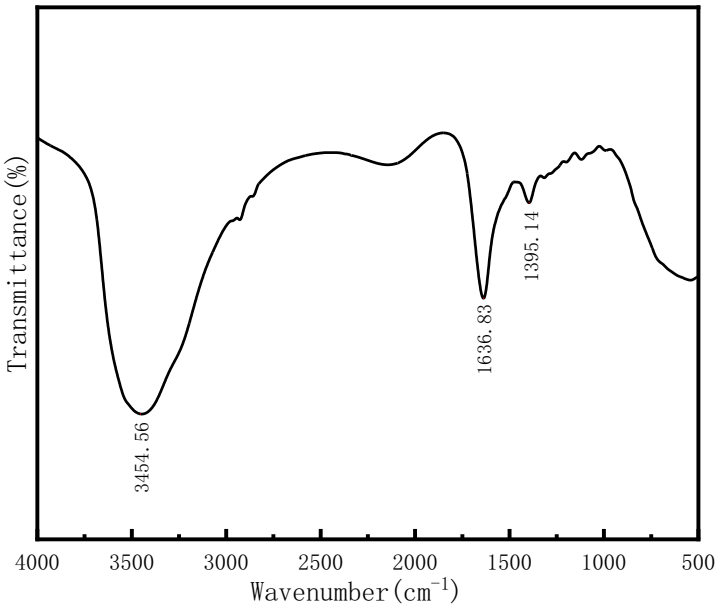

Fig. 6. FTIR of PASP

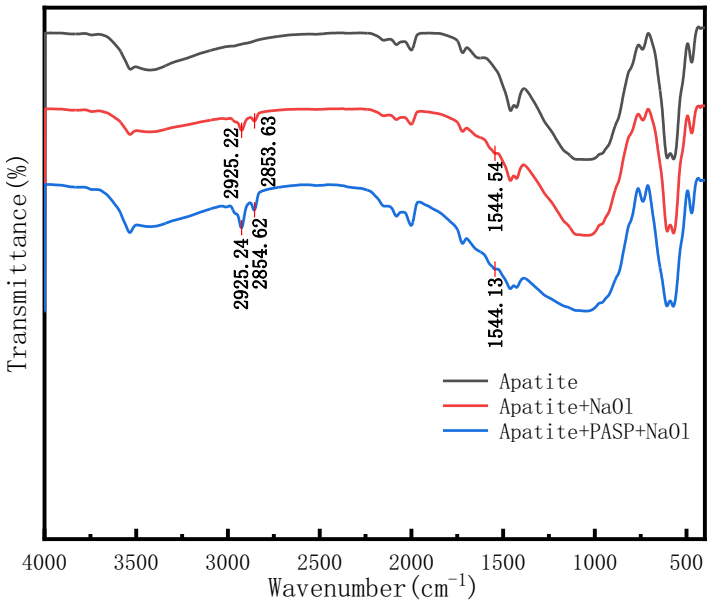

Fig. 7. FTIR of apatite before and after the action of PASP and NaOl

which was due to the stretching vibration of the N-H bond on the amide group (Chen et al.,2020).

The anti-symmetric stretching absorption peak of carboxylic acid with ionic group was found at 1636.82 cm^{-1}, and the peak at 1395.14 cm^{-1} was the symmetric stretching absorption peak of the C=O bond in the carboxylic acid (Zhang et al., 2013). Previous studies have found that NaOl often has spectral peaks caused by asymmetric and symmetric vibration bands containing carboxylic acids at 1560.65 cm^{-1} and 1446.49 cm^{-1}. Also，spectral peaks due to the stretching vibration bands of methyl and methylene are found at 2851.26 cm^{-1} and 2921.31 cm^{-1} (Jiao et al., 2019).

In the presence of NaOl, the FTIR changes of apatite with and without PASP are shown in Fig. 7. For pure apatite, there were no evident characteristic peaks at 2851.26 cm^{-1} and 2921.31 cm^{-1}. When the apatite was treated with NaOl alone, the methyl and methylene stretching vibration bands of NaOl at 2857.30 cm^{-1} and 2922.05 cm^{-1} were more obvious, which illustrated that NaOl was adsorbed on the surface of apatite. The obvious methyl and methylene stretching bands at 2859.37 cm^{-1} and 2926.14 cm^{-1} were showed from PASP pretreated apatite in the presence of NaOl, which indicated that PASP could not hinder the adsorption of NaOl on the surface of apatite pretreated by PASP.

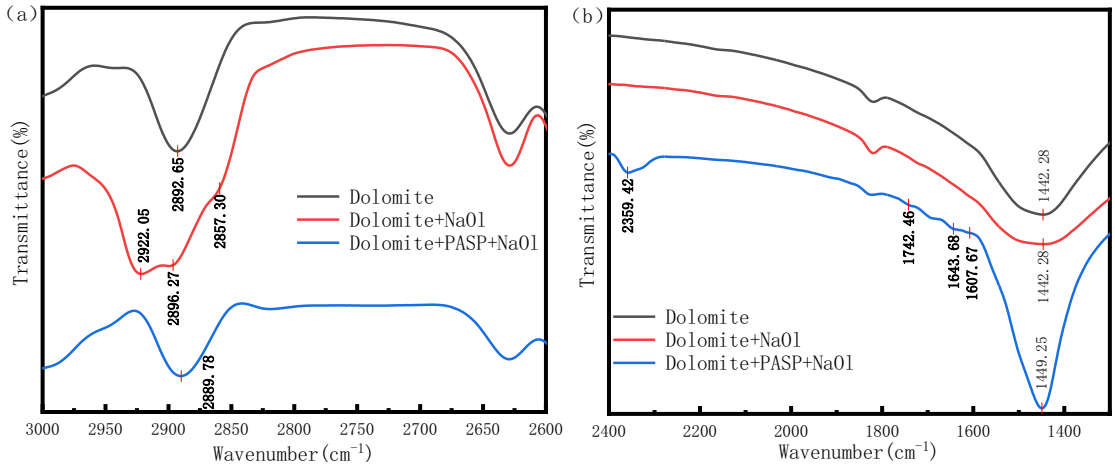

Fig. 8. FTIR of dolomite before and after the action of PASP and NaOl (a) at 2600-3000 cm-1and (b) at 1300-2400 cm-1

Fig. 8 describes the infrared spectrum of dolomite with and without the treatment of agents. The characteristic peaks at 1442.28 cm^{-1} due to the asymmetric stretching vibration of CO_3^{2-} in the spectrum of dolomite. As the dolomite treated with single NaOl, the methyl and methylene stretching vibration bands at 2857.30 cm^{-1} and 2922.05 cm^{-1} were relatively apparent. The other characteristic bands of NaOl, such as 1560.65 cm^{-1} and 1446.49 cm^{-1}, are likely to be covered by the adsorption bands of CO_3^{2-} (Chen et al.,2021). Which indicated that NaOl was adsorbed with a certain degree on the surface of dolomite. When the dolomite was pretreated by PASP, the characteristic peak of NaOl disappeared obviously, revealing that the addition of PASP prevented the adsorption of NaOl on the surface of dolomite (Zeng et al., 2021). In addition, the main characteristic peaks of dolomite pretreated by PASP corresponding to the C=O vibrational adsorption peak of amide group in PASP (1742.46 and 1643.68 cm^{-1}) and C=O vibration couplings of $-COO^-$ group in PASP (1607.67 cm^{-1}) appeared (Wei et al., 2021). It was also apparent to find the N-H Stretching vibration peak of amide group at 2359.42 cm^{-1} (Zeino et al., 2018), which further revealed that PASP was likely to work on the surface of dolomite by chemical adsorption. These conclusions were also consistent with the results of the Zeta potential test.

3.4. XPS analysis

XPS analysis is a significant method of surface element detection, which can provide much information on the surface element composition and chemical state of the sample. The XPS test is used to effectively reveal the mechanism of PASP. The results are shown in Fig. 9-10 and Table 2.

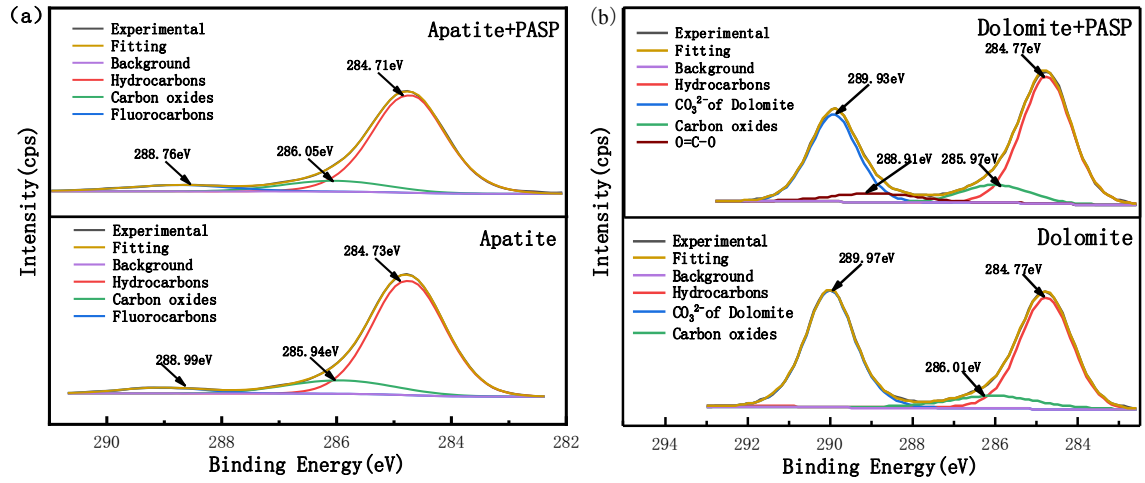

Fig. 9. C1s orbital spectra of apatite (a) dolomite, (b) before and after PASP action

The XPS spectra of carbon and oxygen were separated and fitted. As shown in Fig. 9 (a), the C1s separation peaks at 284.73 eV, 285.94eV and 288.99eV were detected spectral peak of pure apatite, which might be C-C, carbon oxide and fluorocarbon, respectively. The first two characteristic peaks belonged to hydrocarbon and carbon and oxygen pollutants, and the rest was the spectrum peak contained in apatite (Dong et al., 2020). After pre-treatment with PASP, the fluorocarbon peak of apatite had a shift of about 0.23 eV, which illustrated that PASP had a weak impact on the chemical environment of carbon element on the surface of apatite (Nan et al., 2019). As portrayed in Fig. 9 (b), in addition to two common hydrocarbon and carbon oxide peaks appearing at 284.77 eV and 286.01 eV in the C1s spectrum, the separation peak of CO_3^{2-} was also produced at 289.97 eV for untreated dolomite (Yang et al., 2020).After PASP treatment, a new separation peak was found in the C1s spectrum of dolomite at 288.93 eV, which was probably due to the O-C=O produced by the carboxyl group in PASP (Chen et al., 2019).It also revealed that PASP had a significant effect on the chemical environment of carbon element on the surface of dolomite.

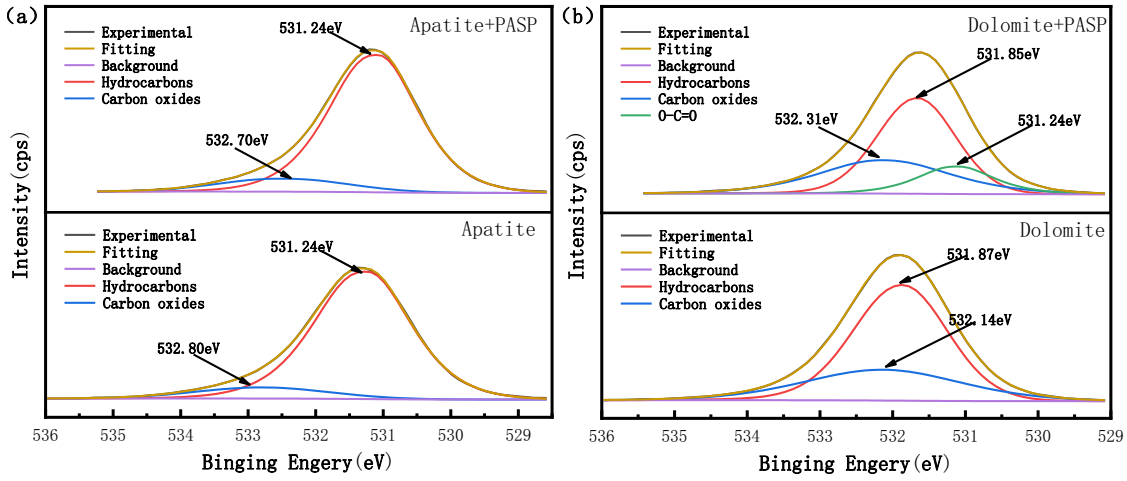

Fig. 10. O1s orbital spectra of apatite (a) dolomite, (b) before and after PASP action

Fig. 10 depicts the O1s spectra of apatite and dolomite with and without the treatment of PASP. As shown in Fig. 10 (a), the O1s separation peaks were detected at 531.24 eV and 532.80 eV for untreated apatite, which were likely to come from the dissolved PO_4^{3-} on the surface of apatite and the adsorbed water, respectively (Filippova et al., 2018). After the treatment of PASP, the separated peaks in the O1s spectrum were basically the same as the fitting peaks of untreated apatite, and no new peaks was found, which illustrated that PASP had a weak effect on the surface of apatite. As depicted in Fig. 10 (b), the well-fitted separation peaks of O1s at 531.87 eV and 532.14 eV were detected for untreated dolomite, which belonged to the oxygen element from CO_3^{2-} in the dolomite and the pollution peak of carbon oxides from foreign material during the preparation process (Deng et al., 2018). The chemical environment on the surface of dolomite had a significant impact with PASP treatment. In addition to the separation peaks of hydrocarbons and carbon oxides at 531.85 eV and 532.31 eV, the O1s peak at 531.24 eV also had a significant peak caused by O-C=O (Martins et al.,2018), which also revealed that PASP had a significant impact on the chemical environment of oxygen element on the surface of dolomite.

From the XPS spectrum fitting analysis, it could be seen that the dolomite pretreated by PASP produced relatively evident new peaks in the O1s and C1s spectra, revealing that PASP generated a strong chemical adsorption on the surface of dolomite. In order to quantitatively analyze the effect of PASP on the surface of dolomite and apatite, Table 2 summarizes the atomic concentration changes of different elements on the surface of dolomite and apatite with and without pretreatment of PASP. It can be known from Table 2 that the carbon atom concentration increased by 5.27% for the dolomite treated with PASP, which illustrated that PASP was adsorbed on the surface of dolomite. It was also detected that the atomic concentration of calcium decreased by 0.74%, and the atomic concentration of magnesium reduced by 1.23%. These discrepancies were probably due to the adsorption of the agent

Table 2. Atomic content and surface element changes of dolomite and apatite

Samples	Elements (at. %)			
	C	O	Ca	Mg
Dolomite	39.09	47.01	9.27	4.63
Dolomite+ PASP	44.36	43.67	8.56	3.40
Changes	5.27	-3.34	-0.74	-1.23
Apatite	29.24	52.68	18.09	-
Apatite+ PASP	28.59	53.34	18.07	-
Changes	-0.65	0.66	-0.02	-

on the surface of dolomite. At the same time, the discrepancy in the concentration of magnesium atoms was higher than the difference in the concentration of calcium atoms, which indicated that PASP mainly had strong chelation with the magnesium ions on the surface of dolomite, and the synergistic effect of metal ions further promoted the adsorption of PASP on the surface of dolomite. On the contrary, the concentration of elements on the surface of apatite changed little. The atomic concentration of carbon reduced by 0.65%, and the atomic concentration of oxygen increased by 0.66%, which was probably due to the dissolved ions on the mineral surface with the action of the PASP. In summary, a large amount of PASP was adsorbed on the surface of dolomite, which weakened the floatability of dolomite, thereby achieving the flotation separation of dolomite and apatite. It further verified the analysis results of infrared spectroscopy and Zeta potential.

3.5. Depression mechanism of HPMA

The distinguishing adsorption characteristics of PASP on the surface of dolomite and apatite are derived from the combined effect of the mineral crystal structure, surface dissolved ion, and the functional groups ionized by PASP. PASP ionizes numerous deprotonated carboxylic acid groups in alkaline solution (Wei et al., 2020), which are inclined to chelate with metal ion on the surface of dolomite and apatite. However, the different crystal structures of the two minerals could lead to the presence of different anionic groups on their surfaces. From the changing trend of Zeta potential, it could be seen that the dissolved phosphate ion on the surface of apatite would generate strong steric hindrance, which would affect the interaction between PASP and calcium ion on the surface of apatite through steric inhibition and repulsion, and it greatly restricted the adsorption of PASP on the surface of apatite (Yang et al., 2021; Chen et al., 2017). On the contrary, the steric hindrance caused by carbonate ion was weak, and the metal ion on the surface of dolomite, especially magnesium ion, were prone to chelating with the carboxylic acid ion in PASP (Jong et al., 2017; Yang et al., 2020). Therefore, PASP was more likely to affect on the surface of dolomite by the means of chemisorption. In addition, PASP and NaOl would have a competitive adsorption on the surface of dolomite and apatite in alkaline slurry. The pre-added PASP would be preferentially adsorbed on the surface of dolomite, which hindered the further adsorption of NaOl, and had a strong inhibitory impact on dolomite. However, the surface of apatite had more calcium ion, which were prone to enhancing adsorption of NaOl so that apatite has good ability of floatability (Ye et al., 2018). Therefore, as shown in Fig. 11, PASP can selectively inhibit dolomite and achieve the flotation separation of dolomite and apatite.

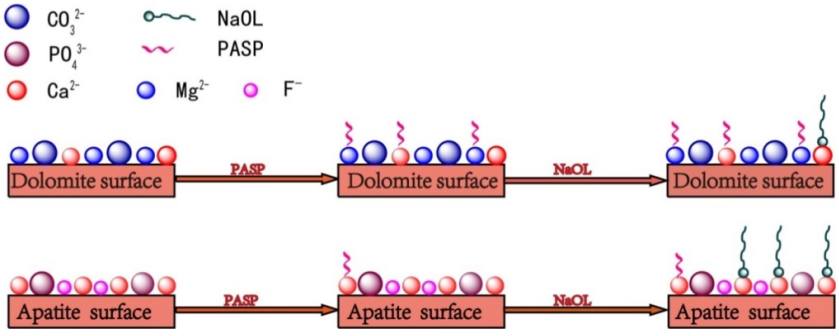

Fig. 11. Schematic diagram of flotation separation of apatite and dolomite

4. Conclusions

PASP was an efficient flotation inhibitor, which could achieve the flotation separation of dolomite and apatite in the range of pH 9-11. When the pH was 10, the flotation recovery of dolomite was reduced to 9.95%, while the flotation recovery of apatite in the presence of PASP was 88.27%. Calcium ions was mainly played a significant role on the surface of apatite, but it was strongly sterically inhibited and repelled by surface anions, which made it difficult for PASP to be absorbed on the surface of apatite. While the exposed ions on the surface of dolomite was magnesium ions and a certain amount of calcium ions from the XPS analysis results, which were more likely to chelate with free carboxyl groups ionized from PASP. These results could be drawn from the difference of the Zeta potential changes of dolomite and apatite before and after PASP pretreatment and changes of infrared spectrum corresponding to PASP, which also revealed that PASP was adsorbed on the surface of dolomite with chemisorption. Therefore, the adsorption effect of inhibitor PASP on the surface of dolomite was much stronger than that of apatite. The difference in adsorption of PASP on the surface of dolomite and apatite could decrease the floatability of dolomite, realizing the separation of the flotation of apatite and dolomite under the NaOl system.

Acknowledgments

This work was financially supported by National Natural Science Foundation of China (51864011); Guizhou Province Science and Technology Plan Project, No.; Qiankehe Platform Talent (2018) No. 5781

References

ABOUZEID, A.M. 2008. *Physical and thermal treatment of phosphate ores – An overview*. Int. J. Miner. Process. 85.

AMIRECH, A., BOUHENGUEL, M., OUACHI, S. 2018. *Two-stage reverse flotation process for removal of carbonates and silicates from phosphate ore using anionic and cationic collectors*. Arab. J. Geosci. 11.

ALINE, P.L.N., ANT, N.E.C.P., ARTHUR, P.C., WANYR, R.F. 2019. *Effect of alkyl chain length of amines on fluorapatite and aluminium phosphates floatabilities.* Journal of Materials Research and Technology 8.

CAO, Q., ZOU, H., CHEN, X., WEN, S. 2019. *Flotation selectivity of N-hexadecanoylglycine in the fluorapatite–dolomite system*. Miner. Eng. 131, 353-362.

CAO, Q., CHENG, J., WEN, S., LI, C., BAI, S., LIU, D. 2015. *A mixed collector system for phosphate flotation*. Miner. Eng. 78, 114-121.

CHEN, C., SUN, W., ZHU, H., LIU, R. 2021. *A novel green depressant for flotation separation of scheelite from calcite*. T. Nonferr. Metal Soc. 31, 2493-2500.

CHEN, C., HU, Y., ZHU, H., SUN, W., QIN, W., LIU, R., GAO, Z. 2019. *Inhibition performance and adsorption of polycarboxylic acids in calcite flotation*. Miner. Eng. 133, 60-68.

CHEN, Q., ZHANG, Q., HART, B.R., YE, J. 2020. *Study on the effect of collector and inhibitor acid on the floatability of collophane and dolomite in acidic media by TOF-SIMS and XPS*. Surf. Interface Anal. 52, 355-363.

CHEN, T., ZENG, D., ZHOU, S. 2018. *Study of Polyaspartic Acid and Chitosan Complex Corrosion Inhibition and Mechanisms*. Pol. J. Environ. Stud. 27, 1441-1448.

CHEN, W., FENG, Q., ZHANG, G., YANG, Q., ZHANG, C. 2017. *The effect of sodium alginate on the flotation separation of scheelite from calcite and fluorite.* Miner. Eng. 113, 1-7.

CHEN, Y., CHEN, X., LIANG, Y. 2020. *Synthesis of polyaspartic acid/graphene oxide grafted copolymer and evaluation of scale inhibition and dispersion performance*. Dlam. Relat. Mater 108, 107949.

CHEN, Y., LONG, Y., LI, Q., CHEN, X., XU, X. 2019. *Synthesis of high-performance sodium carboxymethyl cellulose-based adsorbent for effective removal of methylene blue and Pb (II)*. Int. J. Biol. Macromol. 126, 107-117.

DENG, R., YANG, X., HU, Y., KU, J., ZUO, W., MA, Y. 2018. *Effect of Fe (II) as assistant depressant on flotation separation of scheelite from calcite*. Miner. Eng. 118, 133-140.

DONG, L., WEI, Q., QIN, W., JIAO, F.2020. *Selective adsorption of sodium polyacrylate on calcite surface: Implications for flotation separation of apatite from calcite*. Sep. Purif. Technol. 241.

FILIPPOVA, I.V., FILIPPOV, L.O., LAFHAJ, Z., BARRES, O., FORNASIERO, D. 2018. *Effect of calcium minerals reactivity on fatty acids adsorption and flotation.* Colloids and Surfaces A: Physicochemical and Engineering Aspects 545, 157-166.

GHARABAGHI, M., IRANNAJAD, M., NOAPARAST, M. 2010. *A review of the beneficiation of calcareous phosphate ores using organic acid leaching*. Hydrometallurgy 103, 96-107.

HOANG, D.H., KUPKA, N., PEUKER, U.A., RUDOLPH, M. 2018. *Flotation study of fine grained carbonaceous sedimentary apatite ore – Challenges in process mineralogy and impact of hydrodynamics*. Miner. Eng. 121, 196-204.

HOANG, D.H., HEITKAM, S., KUPKA, N., HASSANZADEH, A., PEUKER, U.A., RUDOLPH, M. 2019. *Froth properties and entrainment in lab-scale flotation: A case of carbonaceous sedimentary phosphate ore*. Chem. Eng. Res. Des. 142, 100-110.

KABA, O.B., FILIPPOV, L.O., FILIPPOVA, I.V., BADAWI, M. 2021. *Interaction between fine particles of fluorapatite and phosphoric acid unraveled by surface spectroscopies*. Powder Technol. 382, 368-377.

LI, X., ZHANG, Q., HOU, B., YE, J., MAO, S. and LI, X. 2017. *Flotation separation of quartz from collophane using an amine collector and its adsorption mechanisms.* Powder Technol 318, 224-229.

LI, X.L.X.B., LIU, Z.L.Z.H., ZHANG, Q.Z.Q., MAO, S.M.S., LI, L.L.L.J. 2014. *The Effect of Ca2+, Mg2+, SO42- and PO43- on Phosphate Ore Flotation.* Advanced Materials Research, 1670-1673.

JIAO, F., DONG, L., QIN, W., LIU, W., HU, C.2019. *Flotation separation of scheelite from calcite using pectin as depressant.* Miner. Eng. 136, 120-128.

JONG, K., HAN, Y., RYOM, S. 2017. *Flotation mechanism of oleic acid amide on apatite*. Colloids and Surfaces A: Physicochemical and Engineering Aspects 523, 127-131.

LIU, X., RUAN, Y., LI, C., CHENG, R. 2017. *Effect and mechanism of phosphoric acid in the apatite/dolomite flotation system*. Int. J. Miner. Process. 167, 95-102.

LIU, X., LUO, H., CHENG, R., LI, C., ZHANG, J. 2017. *Effect of citric acid and flotation performance of combined depressant on collophanite ore*. Miner Eng 109, 162-168.

LIU, Z., SUN, Y., ZHOU, X., WU, T., TIAN, Y., WANG, Y. 2011. *Synthesis and scale inhibitor performance of polyaspartic acid*. J. Environ. Sci.-China 23, S153-S155.

MARTINS, J.G., CAMARGO, S.E.A., BISHOP, T.T., POPAT, K.C., KIPPER, M.J., MARTINS, A.F. 2018. *Pectin-chitosan membrane scaffold imparts controlled stem cell adhesion and proliferation.* Carbohyd. Polym. 197, 47-56.

NAN, N., ZHU, Y., HAN, Y. 2019. *Flotation performance and mechanism of a-Bromolauric acid on separation of hematite and fluorapatite.* Miner. Eng. 132, 162-168.

PAN, Z., WANG, Y., WEI, Q., CHEN, X., JIAO, F., QIN, W. 2020. *Effect of sodium pyrophosphate on the flotation separation of calcite from apatite*. Sep. Purif. Technol. 242, 116408.

RUAN, Y., HE, D., CHI, R. 2019. *Review on Beneficiation Techniques and Reagents Used for Phosphate Ores*. Minerals-Basel 9.

SHAKOOR, M.B., YE, Z., CHEN, S. 2021. *Engineered biochars for recovering phosphate and ammonium from wastewater: A review.* Sci Total Environ 779, 146240.

SIS, H., CHANDER, S. 2003. *Reagents used in the flotation of phosphate ores: a critical review*. Miner. Eng. 16.

SUN, K., LIU, T., ZHANG, Y., LIU, X., WANG, B., XU, C., ZANIN, M. 2017. *Application and Mechanism of Anionic Collector Sodium Dodecyl Sulfate (SDS) in Phosphate Beneficiation*. Minerals-Basel 7.

WANG, J. 2010. *Research and practice of technology of heavy-media separation of collophane*. Huagong Kuangwu Yu Jiagong, 4-6.

WANG, T., FENG, B., GUO, Y., ZHANG, W., RAO, Y., ZHONG, C., ZHANG, L., CHENG, C., WANG, H., LUO, X. 2020. *The flotation separation behavior of apatite from calcite using carboxymethyl chitosan as depressant*. Miner. Eng. 159, 106635.

WANG, X., ZHANG, Q. 2020. *Role of surface roughness in the wettability, surface energy and flotation kinetics of calcite.* Powder Technol. 371, 55-63.

WEI, Q., JIAO, F., DONG, L., LIU, X., QIN, W. 2021. *Selective depression of copper-activated sphalerite by polyaspartic acid during chalcopyrite flotation.* T. Nonferr. Metal Soc. 31, 1784-1795.

WEI, Z., FU, J., HAN, H., SUN, W., YUE, T., WANG, L., SUN, L. 2020. *A Highly Selective Reagent Scheme for Scheelite Flotation: Polyaspartic Acid and Pb-BHA Complexes*. Minerals-Basel 10.

XIE, J., LI, X., MAO, S., LI, L., KE, B., ZHANG, Q. 2018. *Effects of structure of fatty acid collectors on the adsorption of fluorapatite (001) surface: A first-principles calculations*. Appl Surf Sci 444, 699-709.

YANG, B., YIN, W., ZHU, Z., WANG, D., HAN, H., FU, Y., SUN, H., CHU, F., YAO, J. 2019. *A new model for the degree of entrainment in froth flotation based on mineral particle characteristics*. Powder Technol. 354, 358-368.

YANG, B., ZHU, Z., YIN, W., SUN, Q., SUN, H., HAN, H., SHENG, Q., YAO, J. 2020. *Selective adsorption of an eco-friendly and efficient depressant PBTCA onto dolomite for effective flotation of fluorapatite from dolomite*. Chem. Eng. J. 400.

YANG, B., CAO, S., ZHU, Z., YIN, W., SHENG, Q., SUN, H., YAO, J., CHEN, K. 2020. *Selective flotation separation of apatite from dolomite utilizing a novel eco-friendly and efficient depressant for sustainable manufacturing of phosphate fertilizer*. J. Clean. Prod., 124949.

YANG, B., ZHU, Z., SUN, H., YIN, W., HONG, J., CAO, S., TANG, Y., ZHAO, C., YAO, J. 2020. *Improving flotation separation of apatite from dolomite using PAMS as a novel eco-friendly depressant*. Miner. Eng. 156.

YANG, B., YIN, W., ZHU, Z., SUN, H., SHENG, Q., FU, Y., YAO, J., ZHAO, K. 2021. *Differential adsorption of hydrolytic polymaleic anhydride as an eco-friendly depressant for the selective flotation of apatite from dolomite*. Sep. Purif. Technol. 256, 117803.

YANG, L., LI, Y., QIAN, B., HOU, B. 2015. *Polyaspartic acid as a corrosion inhibitor for WE43 magnesium alloy*. Journal of Magnesium and Alloys 3, 47-51.

YE, J., WANG, X., LI, X., MAO, S., SHEN, Z., ZHANG, Q. 2018. *Effect of dispersants on dispersion stability of collophane and quartz fines in aqueous suspensions*. J. Disper. Sci. Technol. 39, 1655-1663.

YE, J., ZHANG, Q., LI, X., WANG, X., KE, B., LI, X., SHEN, Z. 2018. *Effect of the morphology of adsorbed oleate on the wettability of a collophane surface*. Appl. Surf. Sci. 444, 87-96.

YU, H., WANG, H., SUN, C. 2018. *Comparative studies on phosphate ore flotation collectors prepared by hogwash oil from different regions*. International Journal of Mining Science and Technology 28, 453-459.

YU, J., GE, Y., HOU, J. 2016. Behavior and mechanism of collophane and dolomite separation using alkyl hydroxamic acid as a flotation collector. Physicochem. Probl. Mineral Porcess.. 52, 155-169.

ZENG, M., YANG, B., GUAN, Z., ZENG, L., LUO, H., DENG, B. 2021. *The selective adsorption of xanthan gum on dolomite and its implication in the flotation separation of dolomite from apatite*. Appl. Surf. Sci. 551, 149301.

ZEINO, A., ABDULAZEEZ, I., KHALED, M., JAWICH, M.W., OBOT, I.B. 2018. *Mechanistic study of polyaspartic acid (PASP) as eco-friendly corrosion inhibitor on mild steel in 3% NaCl aerated solution*. J. Mol. Liquid 250, 50-62.

ZHANG, Y., ZHU, H., ZHU, J., YANG, F., HE, H., QIN, Z., SHI, Q., PAN, G. 2021. *Experimental and emulational study on the role of ion in coal adsorbing kerosene: Water-kerosene interface and catenoid characteristics*. Fuel 294.

ZHANG, B., ZHOU, D., LV, X., XU, Y., CUI, Y. 2013. *Synthesis of polyaspartic acid/3-amino-1H-1,2,4-triazole-5-carboxylic acid hydrate graft copolymer and evaluation of its corrosion inhibition and scale inhibition performance*. Desallnation 327, 32-38.

ZHONG, B.H, WU, D. Q, YANG, H.L, YANG, X.S., HUANG, M.Y, 2009. *Discussion on the utilization of low-grade phosphate rock in China*. Inorganic Salt Industry 41, 1-5.

ZHOU, F., YANG, L., ZHANG, L., CAO, J., ZHANG, H. 2019. *Investigation of decomposition of dolomite and distribution of iodine migration during the calcination-digestion process of phosphate ore*. Hydrometallurgy 188, 174-181.